Heliyon 8 (2022) e12460

Contents lists available at ScienceDirect

Heliyon

journal homepage: www.cell.com/heliyon

Research article

Utilization of nano volcanic ash as a natural economical adsorbent for removing cadmium from wastewater

Shoroog Alraddadi *

Department of Physics, Umm Al-Qura University, Makkah 24382, Saudi Arabia

ARTICLE INFO

Keywords:
Adsorption
Cadmium
Nano volcanic ash
Pumice
Heavy metals
Aqueous solution
Wastewater

ABSTRACT

The physical properties of volcanic ashes (pumice and scoria) differ based on the locations and historical conditions of the volcanic eruptions, affecting their utilization in applications. In this study, the effectiveness of nano volcanic ash from Al Jabal Al Abyad in eliminating cadmium from aqueous solutions was investigated. Volcanic ash powder was initially milled using a high-energy ball mill to obtain particles with sizes of approximately 500 and 100 nm that were used as adsorbents. The mineralogical and physicochemical properties of the volcanic ash powder were determined using X-ray fluorescence spectroscopy, X-ray diffraction, Raman spectroscopy, and Barrett–Joyner–Halenda analysis. Then, the characteristics of cadmium adsorption (from an aqueous solution) on the volcanic ash powder and nano volcanic ash were determined using atomic absorption spectrophotometry by varying the solution pH, contact time, and initial metal (Cd) ion concentration. Isothermal adsorption and kinetic models were used to determine the analytical potential of the nano volcanic ash. Based on isothermal adsorption analysis, the adsorption capacity increased from 31 to 166 mg/g at pH 6. The adsorption capacity of volcanic ash was much more efficient than that of other natural absorbents owing to its chemical composition, the production of nanoparticles from powdered volcanic ash, and the increase surface area of the adsorbent from 0.293 m^2/g to 20.8735 m^2/g. The results showed that the adsorption process occurred mainly via monolayer adsorption on the homogeneous adsorbent surface, indicating the validity of the Langmuir adsorption isotherm model. The kinetic model showed that the adsorption of Cd on nano volcanic ash followed the pseudo-second-order kinetic model. The adsorption capacity results indicated that nano volcanic ash from Al Jabal Al Abyad is an applicable candidate and economical adsorbent for removing heavy metals such as cadmium from industrial wastewaters.

1. Introduction

In recent years, there has been increasing concern regarding the escalating pollution owing to the emission of heavy metals from municipal and industrial wastewater into the environment [1, 2, 3, 4, 5, 6, 7, 8, 9]. Heavy metals such as cadmium, zinc, mercury, and chromium, which are generally found in industrial wastewater, can pose environment and health hazards [10], leading to diseases such as cancer, cardiovascular disease, and central nervous system dysfunction, even at low concentrations, owing to their bioaccumulation in animal and vegetal populations that constitute aquatic ecosystems, as well as their non-biodegradability [10, 11]. The removal of heavy metals from wastewater is very important for protecting the environment and human health. Thus, several traditional techniques have been used to eliminate these metals from industrial wastewater, including solvent extraction, chemical precipitation, phytoextraction, electrodialysis, ion exchange, membrane filtration, and adsorption [5]. Most of these techniques are not applicable for removing low concentrations of metal ions owing to their high operational cost. Therefore, new low-cost local adsorbents with high adsorption capacity are required for heavy metal removal. Recently, various economical adsorbents that do not require pre-treatment have been efficiently used to eliminate heavy metals from wastewater and aqueous solutions [5, 12, 13, 14, 15, 16, 17, 18, 19]. However, the potential for adsorption depends on many parameters such as the pH, adsorbent dosage, type of heavy metal, surface area, temperature, and contact time. The capacity of previously studied natural adsorbents (such as zeolites, rice husk ash, kaolinite, volcanic ash (pumice or scoria), and perlite) for cadmium removal from aqueous media is presented in Table 1. The data show that natural volcanic materials, such as pumice and nano-pumice, have a maximum adsorption capacity (Q_m) of ~26 and 200 mg/g, respectively, for the removal of heavy metals [6]. Pumice is a type of volcanic ash with high porosity and a large specific

* Corresponding author.
E-mail address: swraddad@uqu.edu.sa.

https://doi.org/10.1016/j.heliyon.2022.e12460
Received 14 July 2022; Received in revised form 13 September 2022; Accepted 8 December 2022

Table 1. Adsorption capacity of different adsorbents from previous studies for removal of cadmium from aqueous solution.

Adsorbent	Maximum adsorption capacity (mg/g)	References
Pumice	26	[6]
Nano-Pumice	200	
Kaolinite	9.9	[15]
Montmorillonite	32.7	
Bentonite	9.3	
Montmorillonite	6.784	[14]
Montmorillonite	0.72	[16]
Kaolinite	0.32	
Zeolite	21.24	[13]
Pumice	8.5	
Diatomite	16.08	[17]
Perlite	0.64	[18]
Rice husk ash	3.02	[19]

surface area of ~2.5–8 m^2/g, with a pH of approximately 7; it is less expensive than other adsorbents [6, 12, 20]. Pumice has been used as a scouring, scrubbing, and polishing material, as well as a construction and pharmaceutical material [21]. Recently, it has been used in water and wastewater purification.

The high SiO_2 and Al_2O_3 content of volcanic materials [22], such as clays and zeolites [23], make them efficient adsorbents. Moreover, their large surface areas [24] endow them with high adsorption ability. Materials with large amounts of silica (SiO_2) and other metal oxides (e.g., Al_2O_3) can eliminate heavy metals from wastewater [25]. However, the physical properties, such as the chemical structure, fineness, specific surface area, and particle size of volcanic ash (pumice and scoria), differ in samples from different locations based on the historical conditions of the volcanic eruptions, which can affect their utilization in applications. The feasibility of using volcanic ash (pumice) from Al Jabal Al Abyad in Saudi Arabia as an adsorbent has not yet been explored. Therefore, this work aims at investigating the effectiveness of volcanic ash specimens from Al Jabal Al Abyad in eliminating cadmium from aqueous solutions. The chemical composition, surface properties, and crystal structures of the pumice specimens were investigated using X-ray fluorescence (XRF), Barrett–Joyner–Halenda analysis, and X-ray diffraction (XRD). The effects of decreasing the particle size of volcanic ash (pumice) to the nano size regime on the adsorption capacity is investigated by varying the cadmium concentration and contact time. The surface characteristics of the nanosized adsorbents prepared using a high-energy ball mill are also determined. High-energy milling has many advantages such as simplicity, low cost, wide-scale applicability, and large-scale production capability [26, 27]. In this technique, powder particles are subjected to repetitive compressive loads by placing them between the contacting surfaces of the balls. Milling induces different effects depending on the nature of the milled materials [28, 29, 30]. Many coexisting ions are present with Cd^{2+} in wastewater; however, this study only focused on the efficiency of removal of Cd^{2+} using nano volcanic ash.

2. Materials and methods

2.1. Preparation of nano volcanic ash specimens

The volcanic ash used in this work was obtained from Al Jabal Al Abyad located in the western region of Saudi Arabia. The raw volcanic ash was milled in two stages in the mineral processing laboratory of the Saudi Geological Survey, Jeddah, Saudi Arabia. In the first stage, the volcanic ash was ground using a crusher unit to obtain a powder

Table 2. Chemical composition of volcanic ash from XRF analysis.

Oxide	SiO_2	Al_2O_3	CaO	Fe_2O_3	K_2O	MgO	MnO	Na_2O	P_2O_5	TiO_2	SO_3	LOI
weight %	71.62	10.87	0.42	3.14	3.62	0.24	0.07	6.08	0.22	0.15	0.05	2.60

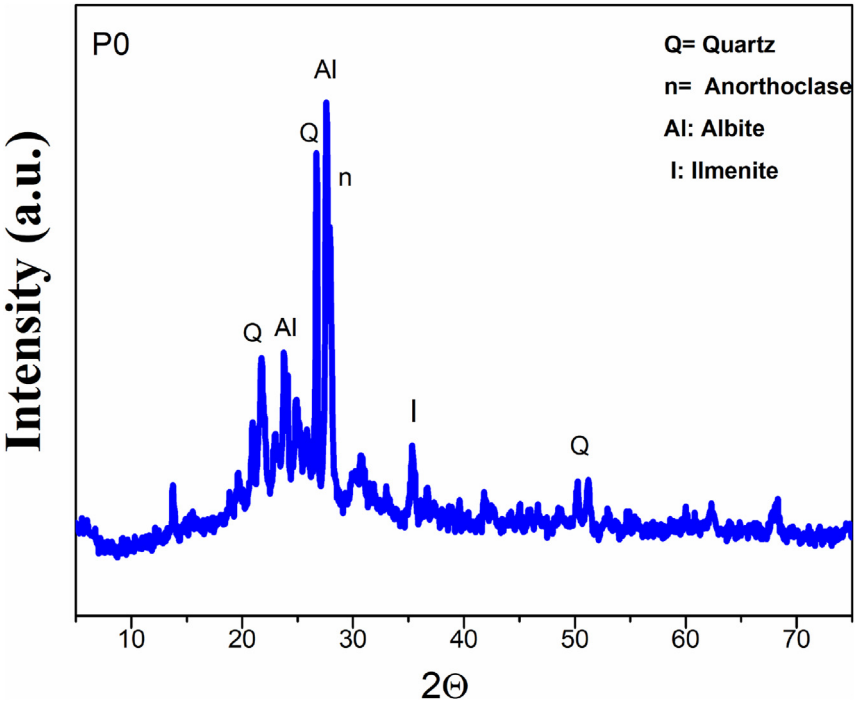

Figure 1. XRD pattern of powdered particles of volcanic ash specimen (P0) before ball milling.

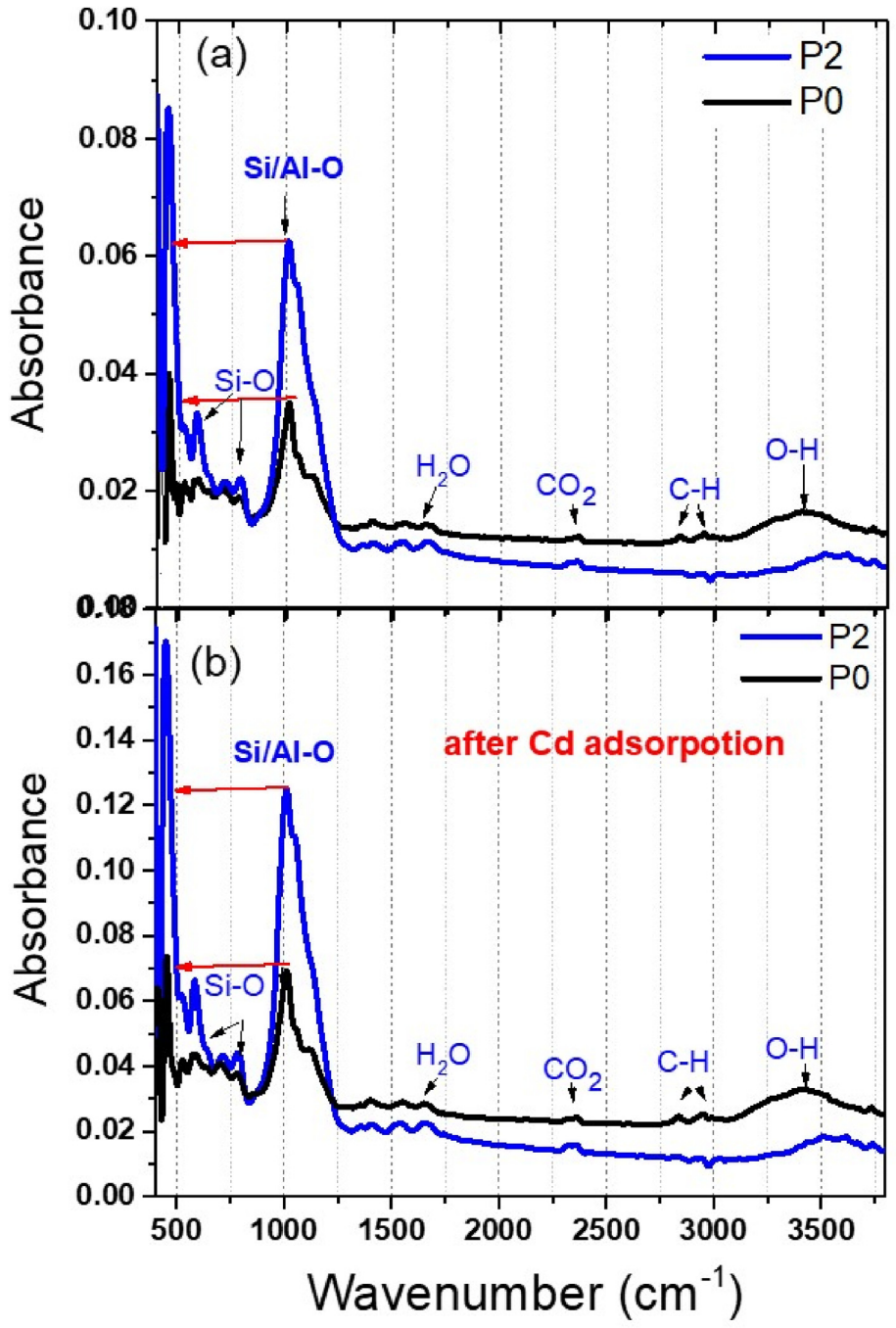

Figure 2. FTIR spectra of powdered volcanic ash (P0) and nano volcanic ash (P2) a) before and b) after the adsorption of cadmium.

with particle sizes less than 5 mm. In the second stage, the ground volcanic ash was processed using a smoothing machine (Pulverizers Agate; ROCKLABS, New Zealand) to form a soft powder. The volcanic ash powder, which was passed through a 200 mesh, was used in high-energy ball milling to prepare nano volcanic ash powder. The powdered volcanic ash (P0) was subjected to high-energy ball milling for different durations at the Center of Excellence in Nanotechnology, King Fahd University of Petroleum & Minerals, Dharan, Saudi Arabia, to obtain two samples (P1 and P2) with respective particle sizes of ~500 and 100 nm. Milling was performed in a 1400 cc jar (container/alumina) at a speed of 3000 rpm, where the ball mill was loaded with a powder-to-ball ratio of 1:20 (50 g of powder to 1 kg of balls (800 μm size)) along with ZrO_2. All three volcanic ash specimens (P0, P1, and P2) were utilized as adsorbents in this study; P0 is the powder volcanic ash specimen, and P1 and P2 are the specimens after high-energy ball milling.

2.2. Preparation of cadmium solutions

Cadmium solutions and standards were prepared using $3CdSO_4{\cdot}8H_2O$. The required amount of Cd(II) salt was solubilized in doubly-distilled water to obtain a 1000 mg/L standard stock solution. Various working standards (25–300 mg/L) were obtained using diluting the stock solution with distilled water; the concentration was measured using an atomic adsorption spectrophotometer. The three volcanic ash specimens (P0, P1, and P2) (100 mg each) were mixed with 50 mL of Cd^{2+} solutions of various concentrations (50, 100, 200, and 300 mg/L) at pH 6 for 60 min to reach an equilibrium. The isothermal adsorption and kinetics were studied using

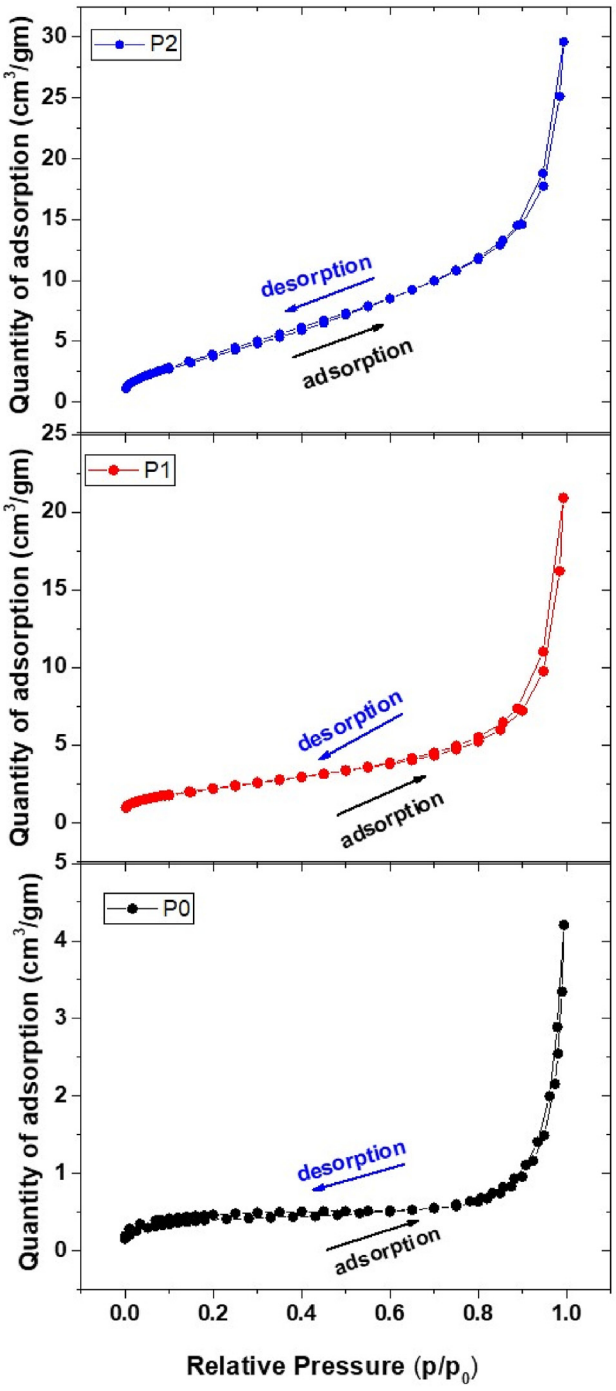

Figure 3. Desorption isotherms of the three volcanic ash powder specimens.

various models. The spent Cd-coated pumice was separated from water by using a filter paper, and it was subsequently treated for reuse in other applications.

2.3. X-ray fluorescence spectroscopy, X-ray diffraction, and FTIR analysis

The chemical composition, as well as the major and minor oxides, of the powder volcanic ash specimen were analyzed using X-ray fluorescence spectroscopy (XRF) (SPECTRO–EXPOS) [31, 32]. A 1 g sample of volcanic ash powder was placed in the platinum crucible and mixed with 8 g of lithium borate, transferred to the fusion system and kept for approximately 20 min, and converted to a glass disk. X-ray diffraction (XRD, Bruker D8 Advance (Bruker, USA)) with Cu-Kα radiation (Kα = 1.54 Å) in the 2θ range of 5–75° was used to determine the phase of the minerals in the volcanic ash specimens [31, 32]. The powder (P0) and nano volcanic ash (P1 and P2) specimens were characterized by Fourier-transform infrared (FTIR) using a Nicolet iS50 FTIR system with a diamond-attenuated total reflection accessory (Thermo Scientific, Massachusetts, USA). The FTIR analysis was performed at room temperature in the range of 4000–400 cm^{-1} to identify the functional groups and adsorbent properties. Focus was placed on the cadmium adsorption ability of the nano volcanic ash samples as a cationic model compound [6, 33, 34, 35].

2.4. Determination of particle size and surface characteristics

The particle sizes of all volcanic ash specimens were measured using a particle size analyzer, at 25 °C. The surface properties of the volcanic ash and nano volcanic ash specimens were determined using the Barrett–Joyner–Halenda (BJH) method [31]. The specific surface area, pore volume, and pore size of the powdered volcanic ash and nano volcanic ash specimens were determined from N_2 adsorption–desorption isotherms at 77 K using a Micromeritics ASAP 2020 instrument. For accurate measurements, the samples were initially degassed under vacuum for approximately 6 h to remove surficial water and other contaminants. Approximately 0.6 g of volcanic ash was placed in a glass tube, degassed, and analyzed using the relevant instrument. The data from this experiment are presented in the form of an isothermal adsorption curve, which delineates the relationship between the quantity of gas adsorbed and the relative pressure.

3. Results and discussion

3.1. XRD, XRF, and FTIR determinations

The XRF data for the volcanic ash specimens are presented in Table 2. The volcanic ash powder consisted mainly of silica (SiO_2) and alumina (Al_2O_3), along with small amounts of calcia (CaO), iron oxide (Fe_2O_3), potassium oxide (K_2O), magnesium (MgO), manganese monoxide (MnO), sodium oxide (Na_2O), phosphorus pentoxide (P_2O_5), titanium dioxide (TiO_2), sulfate (SO_3), and a small proportion of loss on ignition (L.O.I.) that remained in the samples owing to volatile matter from the lower layers of earth. The chemical composition is attributed to the historical conditions of the volcanic eruptions [21, 31, 32, 36]. The high content of SiO_2 and Al_2O_3 on volcanic materials make them efficient adsorbents [22, 23].

Volcanic ash is classified as pumice and scoria depending on the silica content. The specimen contained more than 50% silicon oxide, indicating that it was pumice [21, 31, 32, 36].

Figure 1 displays the XRD pattern of the volcanic ash powder. Both amorphous and crystalline phases were present in the volcanic ash. The

Table 3. Surface parameters and particle size of the volcanic ash specimens.

Surface parameters		Specimen number		
		P0	P1	P2
Surface area (S)	BJH adsorption cumulative surface area (m^2/g)	0.293	7.9113	20.8735
	t-plot external surface area (m^2/g)	0.2558	7.3857	17.3267
Pore volume (V_p)	Pore volume (cm^3/g)	0.00548	0.032279	0.046495
Pore size (d_{av})	Average pore diameter (nm)	74.7660	16.1282	8.9100
Nanoparticle size	Average particle size (nm)	1117	575	100

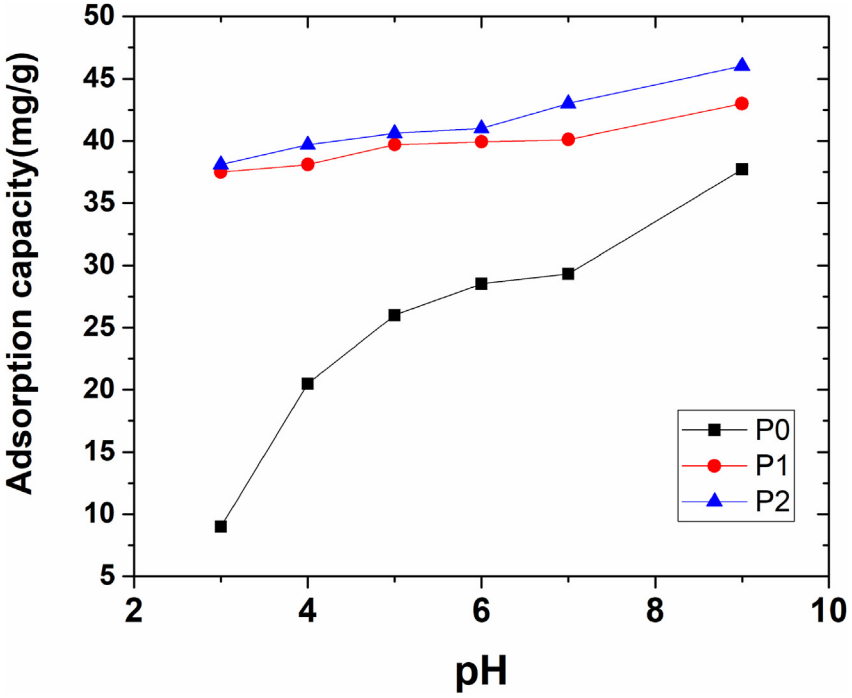

Figure 4. Influence of pH on cadmium adsorption in nano volcanic ash specimens.

volcanic ash (pumice) contained a large quantity of silica in the form of quartz (SiO_2), as well as crystalline minerals such as albite, anorthoclase, and ilmenite [32].

The FTIR spectra of the powder and nano volcanic ash specimens before and after adsorption of Cd were analyzed to investigate the adsorbent properties by focusing on the broad band in the range of 500–900 cm^{-1} (Figure 2(a), (b)), corresponding to the Si–O stretching vibration. The peak at approximately 1012 cm^{-1} is attributed to the Si–O–Al functional groups [37, 38, 39, 40]. The peaks at 3420 and 1650 cm^{-1} are attributed to the presence of silanol (O–H) functional groups and water molecules, respectively [37, 38, 41]. The peaks at 2948–2833 cm^{-1} are related to the stretching vibration of C–H in methane dissolved in the glassy phase, whereas the peak at approximately 2360 cm^{-1} indicates the existence of CO_2 molecules [32, 40].

These results indicate that the particle size decreased and the crystallinity changed upon grinding. The FTIR spectrum of the powdered volcanic ash was the same as that of the nano volcanic ash before the adsorption procedure. Although, the peak intensity for nano volcanic ash decreased in comparison to that of the volcanic ash powder, which corresponded to fewer nano volcanic ash particles. The FTIR spectra of the powder and nano volcanic ash specimens showed the same trend before and after cadmium adsorption; however, the adsorption of Cd led to an increase in the peak intensity owing to the interaction of the functional groups and cadmium ions, as presented in Figure 2(a), (b). The hydroxyl groups [Si (OH)x−n] and [Al (OH)y−m], in the volcanic ash samples are very important for the adsorption of Cd^{2+} ions owing to the tendency of the silicon atoms on the surface groups to undergo tetrahedral coordination with oxygen, enabling them to adsorb positively charged metal ions [6].

3.2. Particle size, surface area, and porosity measurements

The particle sizes of the three volcanic ash specimens were determined using a particle size analysis technique. The surface properties of the ground volcanic ash were evaluated using the Barrett–Joyner–Halenda (BJH) analysis of the desorption isotherm. The experimental isotherms of the three powder volcanic ash specimens are shown in Figure 3. The particle sizes, specific surface areas, total pore volumes, and average pore radius of the adsorbent specimens are listed in Table 3. These properties indirectly affected the adsorption capability of the specimens. Previous studies [6, 41] have shown that increasing the surface area of the material by decreasing the size to the nano level can increase the adsorption capacity.

The analysis showed that the particle size of the powder was 1117 nm. Upon ball milling, the particle size of the volcanic ash decreased to 575 and 100 nm. The specific surface area increased from 0.293 m^2/g for the powdered volcanic ash to 20.8735 m^2/g for the volcanic ash that was ball-milled for 7 h. The specific surface area is a very important factor in determining the efficacy of the materials in several applications, such as water purification, where increasing the surface area of the particles increases their adsorption ability. The pore volumes and average pore diameters of the volcanic ash specimens were in the range of 0.00548–0.046495 $cm^3\ g^{-1}$ and 7.47–8.91 nm, respectively (Table 3).

3.3. Influence of pH

The solution pH is an important factor influencing adsorption efficacy, particularly the adsorption capacity. To determine the influence of pH, 0.1 g of nano volcanic ash was added to 50 ml of cadmium solution (100 mg/l) with various initial pH values (3,4, 5,6, 7, and 9) at room temperature (RT) and agitated at a speed of 500 rpm for 60 min. The adsorption capacity can be determined by applying Eq. (1), where q_e refers to the Cd^{2+} adsorbed by the volcanic ash (mg/g); C_o and C_e are the initial and equilibrium concentrations of Cd^{2+} ions in solution (mg/L), respectively; V is the volume (L); and M is the weight of the volcanic ash (g).

$$q_e = \frac{(C_o - C_e)V}{M} \tag{1}$$

Figure 4 shows the cadmium adsorption capacity of the nano volcanic ash specimens at various pH. The adsorption capacity of the nano volcanic ash specimens for the removal of cadmium ions increased as particle size decreased, irrespective of the pH. Notably, as the pH increased, the adsorption capacity of the P0, P1, and P2 samples increased from 16 to 37.7 mg/g, 37.5–43 mg/g, and 38.1–46 mg/g, respectively. The optimum pH of 6 is close to the natural pH of pumice. Therefore, pH 6 was selected for further experiments in order to avoid the precipitation of insoluble Cd^{2+} hydroxides [6, 18].

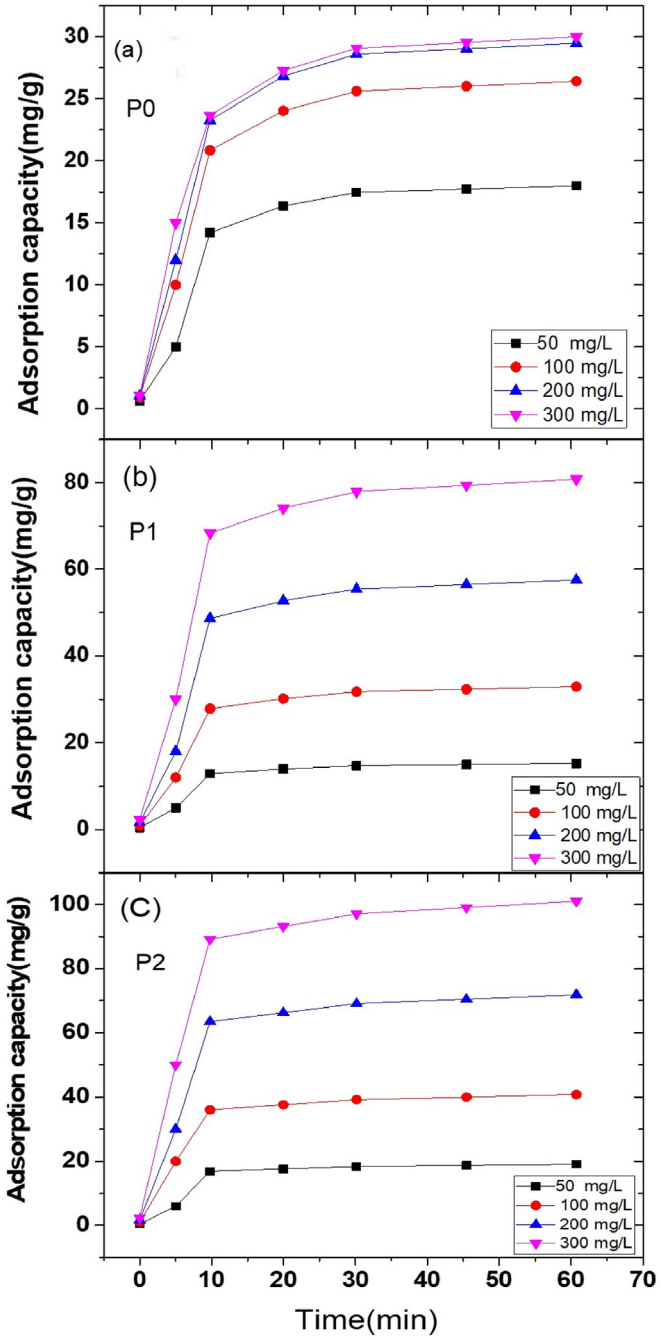

Figure 5. Cadmium adsorption on volcanic ash specimens (P0, P1, and P2) as a function of contact time at pH 6.0 and 25 °C.

3.4. Influence of contact time on Cd adsorption

The adsorption of Cd on the volcanic ash powder (P0) and the ball-milled volcanic ash (P1 and P2) specimens at different Cd concentrations (50, 100, 200, and 300 mg/L) as a function of the contact time are presented in Figure 5(a), (b), and (c). The Cd adsorption capacity of the volcanic ash specimens increased with increasing contact time, where equilibrium conditions were reached within 10 min, after which the state of the system remained constant. This rapid rate of cadmium adsorption in the early period is due to the availability of a large number of vacant adsorption sites on the adsorbent surfaces, whereas as the time increased, the remaining vacancies became occupied [6, 42, 43]. After 60 min, the initial cadmium concentration increased from 50 mg/L to 300 mg/L. The amount of cadmium adsorbed by P0, P1, and P2 increased from 18.1 to 30, 15. 25 to 80.8, and 19.1 to 101, respectively. In other words, with a decrease in the particle size of the volcanic ash, the cadmium adsorption capacity increased owing to the increased surface area of the specimens. This result is consistent with that reported in a previous study [6].

3.5. Adsorption kinetics

Analysis of the adsorption kinetics is an important approach for determining the rate of adsorption of the adsorbate from aqueous solutions and understanding the reaction mechanism. The pseudo-first order and pseudo-second order models were used to determine the rate of adsorption and to evaluate the kinetics parameters [6, 18]. The kinetics data for Cd^{2+} adsorption on nano volcanic ash were investigated using these models. The pseudo first-order and pseudo second-order equations can be expressed using Eqs. (2) and (3), respectively.

$$log(q_e - q_t) = log\, q_e - (k_1 / 2.303)\, t \tag{2}$$

$$\frac{t}{q_t} = \left(\frac{1}{v_O}\right) + \left(\frac{1}{q_e}\right) t \tag{3}$$

where k_1 (1/min) and k_2 (mg/g min) are the rate constants of adsorption for the pseudo first-order and second-order models, respectively; q_e (mg/g) is the quantity of metal ions adsorbed at equilibrium, q_t (mg/g) is the quantity of metal ions on the surface of the adsorbent at time t (min); and $v_O = k_2 q_e^{\ 2}$ is the initial adsorption rate (mg/g min). The kinetics parameters (k_1, k_2) and adsorption capacity (q_e) of nano volcanic ash from the two models were determined from the slope and intercepts of the respective plots of log ($q_e - q_t$) versus t (Figure 6(a)) and t/q_t versus t (Figure 6(b)). The kinetic parameters and correlation coefficients from both models are presented in Table 4. The adsorption kinetics fit well to the pseudo-second-order model (Figure 6(b)). The correlation coefficient for the pseudo-second-order model was higher than 0.99 for cadmium adsorption on all volcanic ash samples (P0, P1, and P2). The theoretical q_e values were close to the experimental q_{exp} values. Therefore, the adsorption of Cd^{2+} on nano volcanic ash follows the pseudo-second order kinetic model. The k_2 values determined from the pseudo-second order kinetics model for Cd adsorption on nano volcanic ash decreased with increasing Cd concentration, indicating that the rate of Cd^{2+} adsorption on nano volcanic ash decreased with increasing Cd concentration. The k_2 values for cadmium adsorption on P1 and P2 nano volcanic ash were lower than 200 mg/L, but they were higher than that of P0, which indicates that P1 and P2 adsorbed Cd ions faster than the P0 sample. This result is in agreement with the result reported in a previous study [6].

3.6. Influence of concentration

The effect of the initial concentration of cadmium on the adsorption capacity of the volcanic ash specimens is presented in Figure 7. When the cadmium concentration was increased from 25 to 300 mg/L, the amount of cadmium adsorbed by the volcanic ash specimen with a size of 1117 nm increased, reaching equilibrium at 30 mg/g, with an initial concentration of 100 mg/L. The quantity of cadmium adsorbed on the volcanic ash specimens with particle sizes of 557 and 100 nm increased from 8.7 to 80.8 mg/g and from 10.9 to 101 mg/g, respectively. However, the adsorption capacity declined, as shown in Figure 8. The high cadmium adsorption percentage achieved with nano volcanic ash at 300 mg/L indicated higher adsorption capability of the nano volcanic ash specimens (P1 and P2) than that of the powder volcanic ash at elevated cadmium concentrations. These obtained results are consistent with those reported previously [6].

3.7. Adsorption isotherm models

The distribution of metal ions between the liquid phase and adsorbent can be described using the Langmuir and Freundlich adsorption isotherm

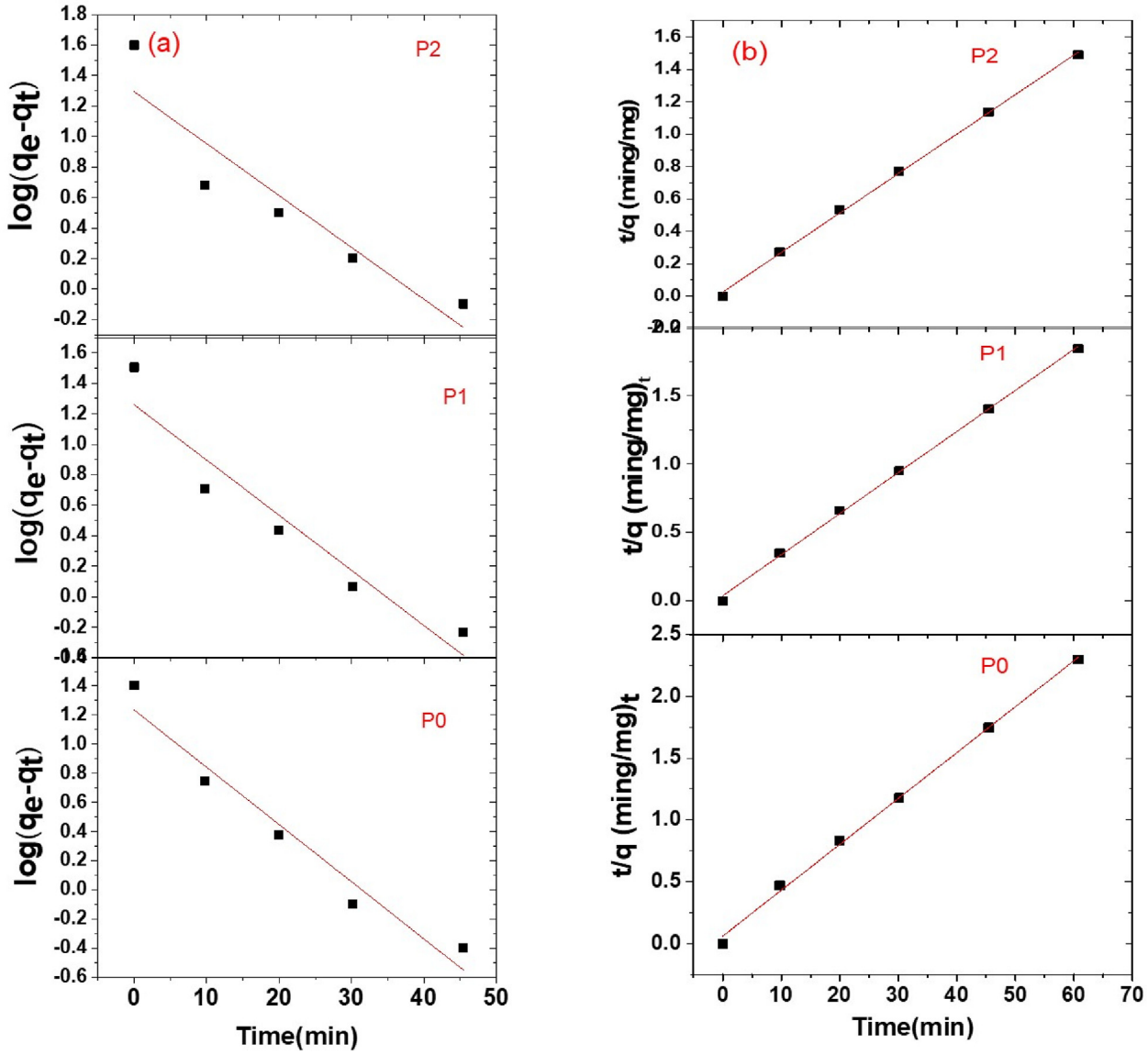

Figure 6. Pseudo (a) first- and (b) second-order adsorption kinetics models of cadmium adsorption on volcanic ash specimens (P0, P1, and P2); initial cadmium concentration = 100 mg/L; pH = 6.0; 25 °C.

Table 4. Kinetic parameters from pseudo first- and second-order models for Cd^{2+} adsorption on the volcanic ash specimens at pH 6.0 and 25 °C.

Sample Number	Initial concentration (mg/L)	q_{exp} (mg/g)	Pseudo first-order			Pseudo second-order		
			q_e (mg/g)	k_1 (1/min)	R^2	q_e (mg/g)	k_2 (g/mg·min)	R^2
P0	50	18	11.66	0.089	0.9774	18.52	0.033	0.9990
	100	26.43	16.98	0.089	0.9774	26.29	0.0235	0.9990
	200	29.5	19.05	0.089	0.9774	30.3	0.02098	0.9990
	300	30	19.50	0.089	0.9774	30.58	0.02096	0.9990
P1	50	15.25	8.39	0.082	0.9587	15.43	0.052	0.9994
	100	32.92	18.19	0.082	0.9587	33.28	0.0242	0.9994
	200	57.51	31.62	0.082	0.9587	58.82	0.013	0.9994
	300	80.8	44.67	0.082	0.9587	81.96	0.009	0.9994
P2	50	19.06	9.12	0.078	0.9334	19.23	0.05	0.9995
	100	40.76	19.498	0.078	0.9334	39.23	0.0255	0.9995
	200	71.88	34.67	0.078	0.9334	72.46	0.014	0.9995
	300	101	47.86	0.078	0.9334	102	0.009	0.9995

Table 5. Langmuir and Freundlich parameters for the adsorption of cadmium by volcanic ash specimens at pH 6.0 and 25 °C.

Type of adsorbent	Langmuir model			Freundlich model		
Sample Number	Q_O (mg/g)	b (l/g)	R^2	n	K_F (l/mg)	R^2
P0	31.27	0.108	0.9999	0.200	$6*10^{-6}$	0.9307
P1	156.25	0.016	0.9230	0.797	0.532	0.9919
P2	166.66	0.006	0.9177	0.695	0.121	0.9816

models, which can be used to evaluate the nature of the adsorption process. These models were used to interpret the equilibrium isotherm data. The Langmuir model of the adsorption process is valid when the adsorption occurs in the homogeneous adsorbent surface using mono-layer sorption. While, the Freundlich model can be applied for non-ideal sorption on heterogeneous surfaces and to multilayer sorption. The Langmuir and Freundlich models can be expressed using Eqs. (4) and (5), respectively.

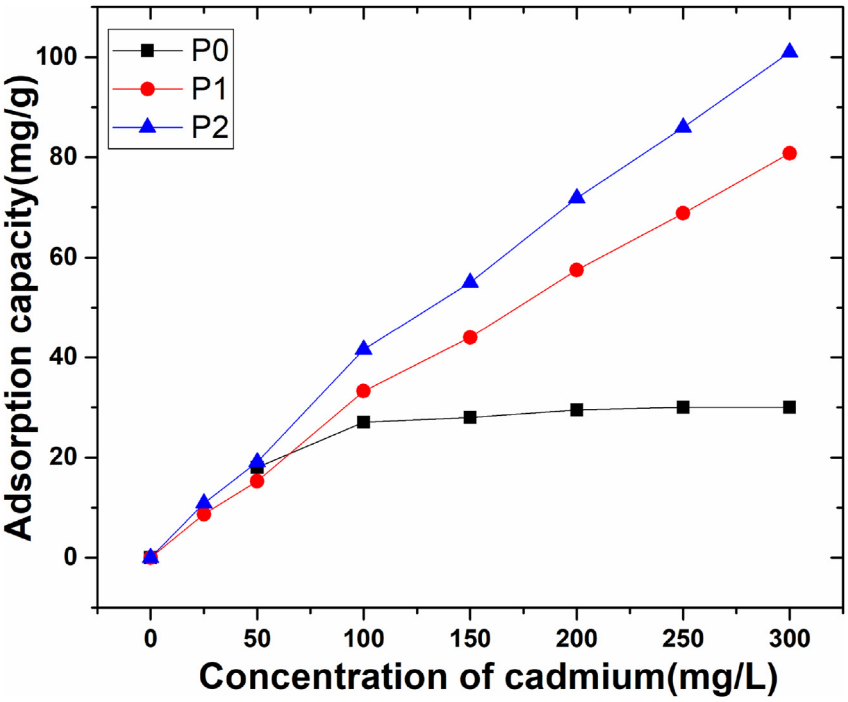

Figure 7. Cadmium adsorption on volcanic ash specimens at different concentrations.

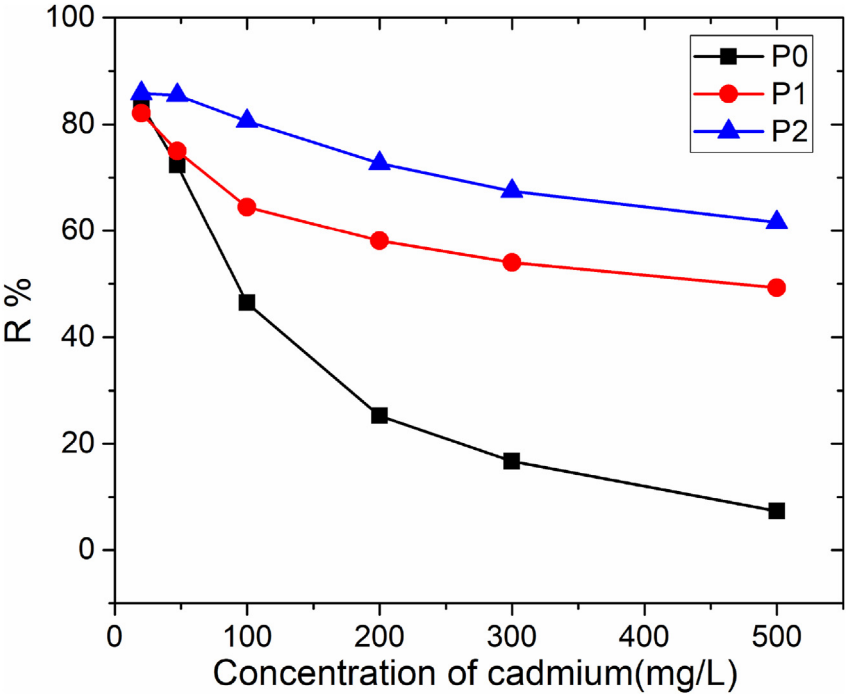

Figure 8. Amount of cadmium adsorbed on volcanic ash specimens at different concentrations.

$$\frac{C_e}{q_e} = \left(\frac{C_e}{Q_O}\right) + 1 \Big/ bQ_O \quad (4)$$

$$q_e = K_F C_e^{1/n} \quad (5)$$

where C_e is the concentration of unadsorbed metal ions in the filtrate (mg/mL) at adsorption equilibrium and q_e is the amount of metal ions adsorbed by the adsorbate (mg/g). Q_o and b are the Langmuir constants for volcanic ash, which Q_o is the maximum cadmium adsorption capacity (mg/g) and b describes the nature of adsorption and the shape of the isotherm (L/mg). K_F is a constant that refers to the adsorption capacity and $1/n$ is an empirical parameter referring to the adsorption intensity, that varies with the heterogeneity of the material. A linear plot of C_e/q_e against C_e gives a straight line with a slope of $1/Q_o$ and an intercept of $1/Q_o{\cdot}b$. The Freundlich parameters K_F and n can be determined from the intercept and slope of the linear plot of log (q_e) versus log (C_e). The Langmuir adsorption isotherm model can also be described using the equilibrium parameter, R_L expressed by Eq. (6).

$$R_L = \frac{1}{(1 + bC_o)} \quad (6)$$

The adsorption isotherm data strongly support monolayer adsorption on a homogeneous adsorbent surface, as the main process (see Table 5). Based on the Langmuir model, the maximum Cd^{2+} adsorption capacity of the P0, P1, and P2 samples was 31.27, 156.25, and 166.66 mg/g, respectively, which presents the potential applicability of P2 for the removal of Cd^{2+} ions from aqueous solutions. This result may be due to the increase in the surface area along with the decrease the particle size because the ability of adsorption increases with increasing the surface area of the particles [6]. However, the maximum capacity for Cd^{2+} adsorption in this work is larger than the maximum adsorption capacities of different adsorbents that reported in previous studies [13, 14, 15, 16, 17, 18, 19]. On the other hand, it was reported in earlier studies by Khorzughy et al. [6] that the maximum capacity for Cd^{2+} adsorption using nano-pumice was 200 (mg/g) which is larger than the maximum adsorption capacity for this study. The Langmuir correlation coefficient (R^2) of 0.99–0.92 for the adsorption of Cd^{2+} on the volcanic ash samples of this study, indicates that the Langmuir model effectively describes the adsorption of Cd^{2+}. Moreover, the R_L value for Cd adsorption onto volcanic ash was between 0 and 1. Along with the type of isotherm, these values support a highly favorable adsorption process according to the Langmuir model. The n value for Cd adsorption on all volcanic ash samples was lower than 1, indicating an unfavorable adsorption process based on the Freundlich model. This result is not consistent with that reported a previously [6], which showed that the Cd adsorption on nano-pumice followed the Freundlich model ($R^2 = 0.9939$).

4. Summary

The efficiency of cadmium removal from aqueous solution was investigated using nano volcanic ash from Al Jabal Al Abyad with particle sizes of approximately 500 and 100 nm. Volcanic ash was subjected to high-energy ball milling to obtain nanosized powder with large specific surface area and high adsorption efficiency. The adsorption of Cd (from aqueous solution) on the nano volcanic ash powder was characterized using atomic absorption spectrophotometry by varying the pH, contact time, and initial metal (Cd) ion concentration. From all measurements, the following significant conclusions can be drawn.

i. XRF analysis showed that the volcanic ash (pumice) consisted mainly of silica and alumina along with small amounts of other oxide metals. The high content of SiO_2 and Al_2O_3 makes the volcanic ash efficient adsorbent.
ii. The XRD pattern of the volcanic ash powder displayed both amorphous and crystalline phases, which contained a large quantity of silica in the form of quartz as well as crystalline minerals such as albite, anorthoclase, and ilmenite.
iii. Surface property measurements revealed that the specific surface area of volcanic ash increased from 0.293 m^2/g for powdered volcanic ash (P0) to 20.8735 m^2/g for the volcanic ash sample (P2) obtained after 7 h of ball milling.
iv. The results of the adsorption experiments showed that the amount of Cd adsorbed by volcanic ash increased with increasing pH, and the optimum pH was 6.0.
v. The cadmium-nano volcanic ash systems attained equilibrium within 10 min.
vi. Isothermal studies showed that the adsorption of Cd on nano volcanic ash follows the Langmuir model.
vii. The data obtained from the Cd adsorption kinetic studies best fit the pseudo-second-order kinetic model.
viii. The maximum capacity of the volcanic ash samples increased as the particle size decreased to the nano level, where the Cd adsorption capacity increased from 31 to 166 mg/g for the P0 and P2 samples, respectively.
ix. The efficient adsorption capacity of volcanic ash nanoparticles from Al Jabal Al Abyad makes it a promising low-cost and suitable adsorbent material for removing Cd from industrial wastewater.

Declarations

Author contribution statement

Shoroog Alraddadi: Conceived and designed the experiments; Performed the experiments; Analyzed and interpreted the data; Contributed reagents, materials, analysis tools or data; Wrote the paper.

Funding statement

This research did not receive any specific grant from funding agencies in the public, commercial, or not-for-profit sectors.

Data availability statement

Data will be made available on request.

Declaration of interest's statement

The authors declare no competing interests.

Additional information

No additional information is available for this paper.

Acknowledgements

The Saudi Geological Survey, the Center of Nanotechnology at King Fahd University of Petroleum & Minerals, and the Center of Excellence in Environmental Studies at King Abdul-Aziz University are acknowledged for their technical support to perform this work.

References

[1] H. Liang, H. Esmaeili, Application of nanomaterials for demulsification of oily wastewater: a review study, Environ. Technol. Innovat. 22 (2021), 101498.
[2] L. Yao, A. Selmi, H. Esmaeili, A review study on new aspects of biodemulsifiers: production, features and their application in wastewater treatment, Chemosphere 284 (2021), 131364.
[3] X. He, T. Zhang, Q. Xue, Y. Zhou, H. Wang, N.S. Bolan, R. Jiang, D.C. Tsang, Enhanced adsorption of Cu(II) and Zn(II) from aqueous solution by polyethyleneimine modified straw hydrochar, Sci. Total Environ. 778 (2021), 146116.
[4] S. Tamjidi, B.K. Moghadas, H. Esmaeili, F.S. Khoo, G. Gholami, M. Ghasemi, Improving the surface properties of adsorbents by surfactants and their role in the

removal of toxic metals from wastewater: a review study, Process Saf. Environ. Protect. 148 (2021) 775–795.
[5] V.K. Gupta, C.K. Jain, I. Ali, M. Sharma, V.K. Saini, Removal of cadmium and nickel from wastewater using bagasse fly ash—a sugar industry waste, Water Res. 37 (2003) 4038–4044.
[6] S.H. Khorzughy, T. Eslamkish, F.D. Ardejani, M.R. Heydartaemeh, Cadmium removal from aqueous solutions by pumice and nano-pumice, Kor. J. Chem. Eng. 32 (2015) 88–96.
[7] A.K. Priya, V. Yogeshwaran, S. Rajendran, T.K. Hoang, M. Soto-Moscoso, A.A. Ghfar, C. Bathula, Investigation of mechanism of heavy metals (Cr^{6+}, Pb^{2+} & Zn^{2+}) adsorption from aqueous medium using rice husk ash: kinetic and thermodynamic approach, Chemosphere 286 (2022), 131796.
[8] I. Rabani, R. Zafar, K. Subalakshmi, H.S. Kim, C. Bathula, Y.S. Seo, A facile mechanochemical preparation of Co_3O_4@g-C_3N_4 for application in supercapacitors and degradation of pollutants in water, J. Hazard Mater. 407 (2021), 124360.
[9] L.M.B. Moungam, K.V. Tchieda, H. Mohamed, N.C. Pecheu, R.C. Kaze, E. Kamseu, I.K. Tonle, Efficiency of volcanic ash-based porous geopolymers for the removal of Pb^{2+}, Cd^{2+} and Hg^{2+} from aqueous solution, Cleaner Mater 5 (2022), 100106.
[10] E.M. Alissa, G.A. Ferns, Heavy metal poisoning and cardiovascular disease, J. Toxicol. 2011 (2011) 1–2.
[11] C.V. Mohod, J. Dhote, Review of heavy metals in drinking water and their effect on human health, Int. J. Innovative. Res. Sci. Eng. Technol. 2 (7) (2013) 2992–2996.
[12] M. Tapan, T. Depci, A. Özvan, T. Efe, V. Oyan, Effect of physical, chemical and electro-kinetic properties of pumice on strength development of pumice blended cements, Mater. Struct. 46 (10) (2013) 1695–1706.
[13] M.R. Panuccio, A. Sorgona, M. Rizzo, G. Cacco, Cadmium adsorption on vermiculite, zeolite and pumice: batch experimental studies, J. Environ. Manag. 90 (1) (2009) 364.
[14] A. Sdiri, T. Higashi, T. Hatta, F. Jamoussi, N. Tase, Evaluating the adsorptive capacity of montmorillonitic and calcareous clays on the removal of several heavy metals in aqueous systems, Chem. Eng. J. 172 (1) (2011) 37.
[15] K.G. Bhattacharyya, S.S. Gupta, Adsorption of a few heavy metals on natural and modified kaolinite and montmorillonite: a review, Adv. Colloid Interface Sci. 140 (2) (2008) 114.
[16] S. Babel, T.A. Kurniawan, Low-cost adsorbents for heavy metals uptake from contaminated water: a review, J. Hazard Mater. 97 (1–3) (2003) 219.
[17] M.A.M. Khraisheh, Y.S. Al-Degs, W.A.M. Mcminn, Remediation of wastewater containing heavy metals using raw and modified diatomite, Chem. Eng. J. 99 (2) (2004) 177.
[18] T. Mathialagan, T. Viraraghavan, Adsorption of cadmium from aqueous solutions by perlite, J. Hazard Mater. 94 (3) (2002) 291.
[19] V.C. Srivastava, I.D. Mall, I.M. Mishra, Competitive adsorption of cadmium(II) and nickel(II) from aqueous solution onto rice hush ash, Chem. Eng. Process 48 (2009) 370–379.
[20] E. Alemayehu, B. Lennartz, Adsorptive removal of nickel from water using volcanic rocks, Appl. Geochem. 25 (2010) 1596–1602.
[21] P.N. Lemougna, K.T. Wang, Q. Tang, A.N. Nzeukou, N. Billong, U.C. Melo, X.M. Cui, Review on the use of volcanic ashes for engineering applications, Resour. Conserv. Recycl. 137 (2018) 177–190.
[22] A. Alemu, B. Lemma, N. Gabbiye, M.T. Alula, M.T. Desta, Removal of chromium (VI) from aqueous solution using vesicular basalt: a potential low cost wastewater treatment system, Heliyon 4 (7) (2018), e00682.
[23] S. Salamah, The characterization of Merapi volcanic ash as adsorbent for dyes removal from batik wastewater, Key Eng. Mater. 718 (2017) 196–200.
[24] Y. Pratama, H.T. Putranto, Coal Fly Ash Conversion to Zeolite for Removal of Chromium and Nickel from Wastewaters, Doctoral Dissertation, Thesis Program Pascasarjana ITB, Central Library Institute Technology Bandung), 2007.
[25] P. de Rozari, D.S. Krisnayanti, K.V. Yordanis, M.R.R. Atie, The use of pumice amended with sand media for domestic wastewater treatment in vertical flow constructed wetlands planted with lemongrass (Cymbopogon citratus), Heliyon 7 (7) (2021), e07423.
[26] C.C. Koch, Top-down synthesis of nanostructured materials: mechanical and thermal processing methods, Rev. Adv. Mater. Sci. 5 (2003) 91–99.
[27] V.G. Sree, C. Bathula, A.N. Kadam, M.K. Ravindra, K.M. Mahadevan, J.I. Sohn, H. Im, Halogen-free solvent processed light-emitting diodes achieving EQE of nearly 25% for imidazole-based host materials synthesized by ball milling, Nano Energy 92 (2022), 106753.
[28] G.M. Chow, L.K. Kurihara, in: C.C. Kock (Ed.), Chemical Synthesis and Processing of Nanostructured Powders and Films, Nanostructured Materials: Processing, Properties and Potential Applications, Noyes Publications, Norwich, 2002.
[29] S. Doppiu, V. Langlais, J. Sort, S. Suriñach, M.D. Baro, Y. Zhang, G. Hadjipanayis, J. Nogués, Controlled reduction of NiO using reactive ball milling under hydrogen atmosphere leading to Ni− NiO nanocomposites, Chem. Mater. 16 (2004) 5664–5669.
[30] A.S. Bolokang, M.J. Phasha, Thermal analysis on the curie temperature of nanocrystalline Ni produced by ball milling, Adv. Powder Technol. 22 (2011) 518–521.
[31] S. Alraddadi, H. Assaedi, Physical properties of mesoporous scoria and pumice volcanic rocks, J. Phys. Commun. 5 (2021), 115018.
[32] S. Alraddadi, H. Assaedi, Characterization and potential applications of different powder volcanic ash, J. King Saud Univ. Sci. 32 (2020) 2969–2975.
[33] Y.F. Lin, H.W. Chen, P.S. Chien, C.S. Chiou, C.C. Liu, Application of bifunctional magnetic adsorbent to adsorb metal cations and anionic dyes in aqueous solution, J. Hazard Mater. 185 (2011) 1124–1130.
[34] S.H. Huang, D.H. Chen, Rapid removal of heavy metal cations and anions from aqueous solutions by an amino-functionalized magnetic nano-adsorbent, J. Hazard Mater. 163 (2009) 174–179.
[35] G.J. Churchman, W.P. Gates, B.K.G. Theng, G. Yuan, in: F. Bergaya, K.G.T. Benny, G. Lagaly (Eds.), Clays and clay Minerals for Pollution Control. Developments in Clay Science, Edtied, 1, Elsevier, 2006, pp. 625–675.
[36] S. Alraddadi, Surface and thermal properties of fine black and white volcanic ash, Mater. Today Proc. 26 (2020) 1964–1966.
[37] J.N.Y. Djobo, A. Elimbi, H.K. Tchakouté, S. Kumar, Reactivity of volcanic ash in alkaline medium, microstructural and strength characteristics of resulting geopolymers under different synthesis conditions, J. Mater. Sci. 51 (2016) 10301–10317.
[38] Z. Huang, Z. Wang, F. Chen, Q. Shen, L. Zhang, Band structures and optical properties of Al-doped α-Si3N4: theoretical and experimental studies, Ceram. Int. 42 (2016) 3681–3686.
[39] H.K. Tchakouté, S. Kong, J.N.Y. Djobo, L.N. Tchadjié, D. Njopwouo, A comparative study of two methods to produce geopolymer composites from volcanic scoria and the role of structural water contained in the volcanic scoria on its reactivity, Ceram. Int. 41 (2015) 12568–12577.
[40] G. Fine, E. Stolper, Dissolved carbon dioxide in basaltic glasses: concentrations and speciation, Earth Planet Sci. Lett. 76 (1986) 263–278.
[41] R.P.H. Gasser, An Introduction to Chemisorption and Catalysis by Metal, Clarendon Press, Oxford, 1985.
[42] B. Al-Rashdi, C.H. Tizaoui, N. Hilal, Copper removal from aqueous solutions using nano-scale diboron trioxide/titanium dioxide (B2O3/TiO2) adsorbent, Chem. Eng. J. 183 (2012) 294.
[43] I.Y. Rushdi, El-E. Bassam, H. Ala'a Al-Muhtaseb, Adsorption characteristics of natural zeolites as solid adsorbents for phenol removal from aqueous solutions: kinetics, mechanism, and thermodynamics studies, Chem. Eng. J. 171 (3) (2011) 1143.